Tuijin Jishu/Journal of Propulsion Technology
ISSN: 1001-4055
Vol. 45 No. 4 (2024)

Optimization and Performance Analysis of Grid-Connected Hybrid Energy Systems Using Machine Learning in a Commercial Building

S. Parameswari*, V. Suresh Kumar

Department of EEE, Thiagarajar College of Engineering, Madurai-625015, Tamil Nadu, India.

*Corresponding author details,jebamjeeva@gmail.com

Abstract

In this study, grid-dependent hybrid energy systems in a variety of combinations are examined in order to supply dependable power to a commercial structure edge matrix multinational company is located in Madurai, Tamil Nadu, India. The primary objective of the study is to analyze details about a hybrid energy system design that includes conversion, battery packs, a generator powered by diesel, and sunlight harvesting panels. This study took into account both technical and economic factors in order to observe the best design. The Homer tool is used in the present investigation to gather energy price and renewable fraction information regarding the office structure source details under consideration. To confirm its effectiveness, the regression model was contrasted with three evaluation matrices of 27 prediction models with relation to techno-economic aspects. Finally, the findings reveals that optimal configuration and model of this considered locale is Battery. Grid and solar.In terms of LCOE and renewable fraction the optimizable GPR model is outperforms the other model.

1 Introduction

Implementing sources of clean power has garnered a lot of attention recently because of its ability to alleviate issues brought on by the impact of climate change the need for clean energy [1]. The infrastructure for clean and sustainable energy now depends heavily on green power. Meanwhile, the sporadic and unexpected character of this renewable energy prevents its broad use[2]. Lessening the effects of this intermittent issue, resulting in more consistent power generation with fewer fluctuations in electrical frequency and voltage [3]. Power sectors are now a practical way to facilitate the use of green power in the construction sector [4]. using solar energy, wind farms, and storage batteries to power homes and found that more than half of the energy came from renewable sources[5]. The HRES reduces the uncertainty that comes with depending just on one green power source by allowing the integration of multiple sources of green electricity [6].Additionally, green communities offer substantial ecological benefits like reduced greenhouse gas emissions, improved air quality, and increased resistance to the effects of changes in the climate [7]. Maximizing the use of renewable energy sources and achieving the most feasible balance of power are essential for optimizing a power community [8]. Environmental pollution and the possibility of power crises are two negative effects of this growing demand for energy. The burning of coal and petroleum to generate power is one of the main causes of air pollution [9]. Recent years have seen a notable acceleration of the use of sources of clean energy (RE), due to rising demand for energy worldwide and growing concerns of environmental issues [10]. The installation of rooftop photovoltaic arrays in dwellings in Saudi Arabia has a major impact on the management of energy, according to the outcomes. An investigation of an affordable HRES intended to meet the energy needs of rural South African communities has concluded [11]. In order to ensure that there is no possibility of electrical power outage (LPSP), the researchers employ the HOMER approach to determine the most optimal configuration. Moreover, a techno-economic assessment of an integrated solar power (HRE) system is created to help electrify Korkadu village, employing ANN with Back propagation to lower the COE and NPC [12]. Suggested a machine learning

method to control the power of the intelligent grid's clean power sector [13]. The optimal HRE system capacity is determined by forecasting load demand fluctuation using machine learning methods [14]. In a recent work, an integrated approach relying on the marine predator optimization algorithm (MPA) and reinforcement learning (RL) was developed for the best possible configuration of an integrated system that includes a diesel generator, battery (BAT) storage, PV, and WT [15]. Quick convergence rates, reliable outputs, and less computational work are characteristics of mixed metaheuristic techniques [16].A model built using machine learning is a good way to evaluate the efficacy of HRES configurations. medical assessment [17].In [18], a system using AI was introduced to manage electricity for city's infrastructure with photovoltaic and BESS equipment.

1.1 Novelty and contribution

The study examines several configurations of grid-tied hybrid renewable energy systems (HRES) to supply power to a business facility at Edge matrix corporation company in Tamil Nadu, India. The previous debate and the findings of a recent study make it abundantly evident that the majority of scholars have put an effective attention to HRES's financial and technical evaluation.

The present research's contributions are as follows:

- Identified the optimal structure by carefully weighing the various combinations while accounting for ecological, budgetary, and technological considerations.
- Data collected from HOMER Pro tools to forecast the effectiveness of the system using 27 regression machine learning algorithms.
- The study has also identified the best approach to system framework for predicting the financial and technological factors.

2 Current state of the system

2.1 Test Locale

The chosen site of the HES study is Edge matrix multi -national company. madurai, Tamil-nadu india .Its coordinates are 09º54’26.28’ N and 78º 06’51.84° E. The working hours of this company is from dawn at 9am and dusk at 7pm.The maximum demand of this company is 16kVA.which is shown in figure.1.

2.2 Daily load profile

This figure 2 shows the daily load profile of the Edge matrix Multi National company, Madurai, Tamil Nadu ,India. The x-axis represents the time in hours and y-axis represents the power in kW. The working hours of the office at 9am to 7pm.This figure is obtained by using Homer Pro tool and its hourly variation is to optimize the system performance.

Fig.1Arial view of test locale

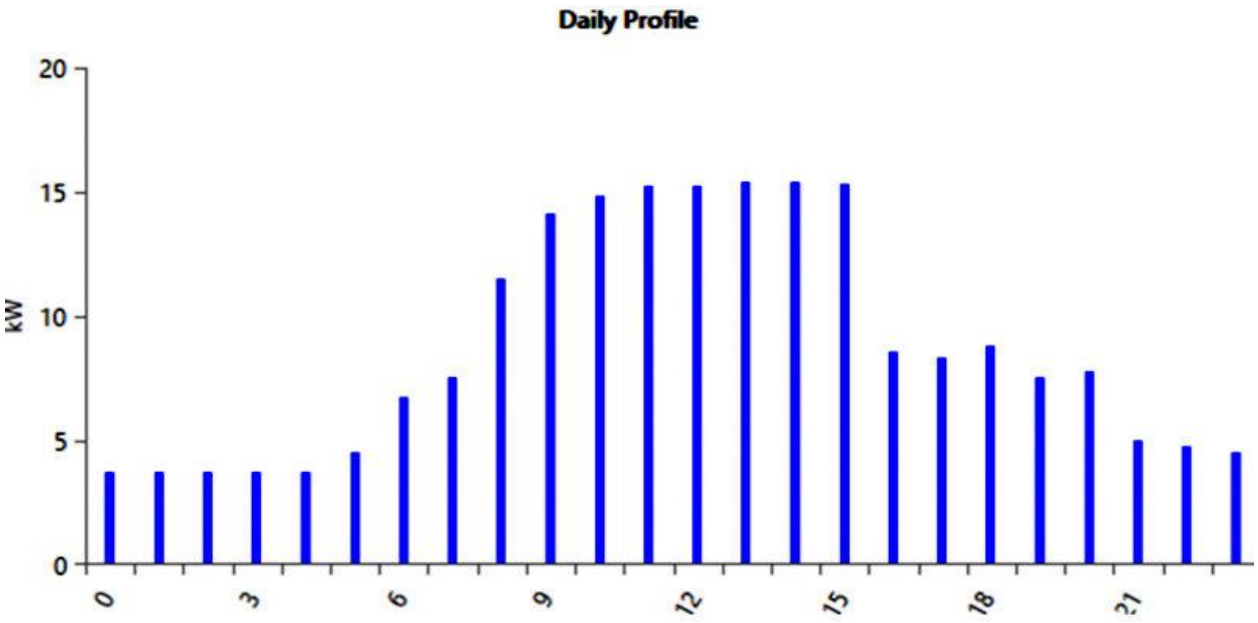

Fig.2 Daily load pattern of the test system

2.3 Seasonal Profile

This figure 3 shows the monthly variation of power over the year. The x-axis represents the monthly variation over the year and y-axis represents the power in kW. From this plot ,it can be observed that mostly median power values are remain same throughout the year. There is no seasonal fluctuation over the year but with minor monthly variation occurred. It's very useful for understanding the long-term system performance and also to allocate the resources effectively

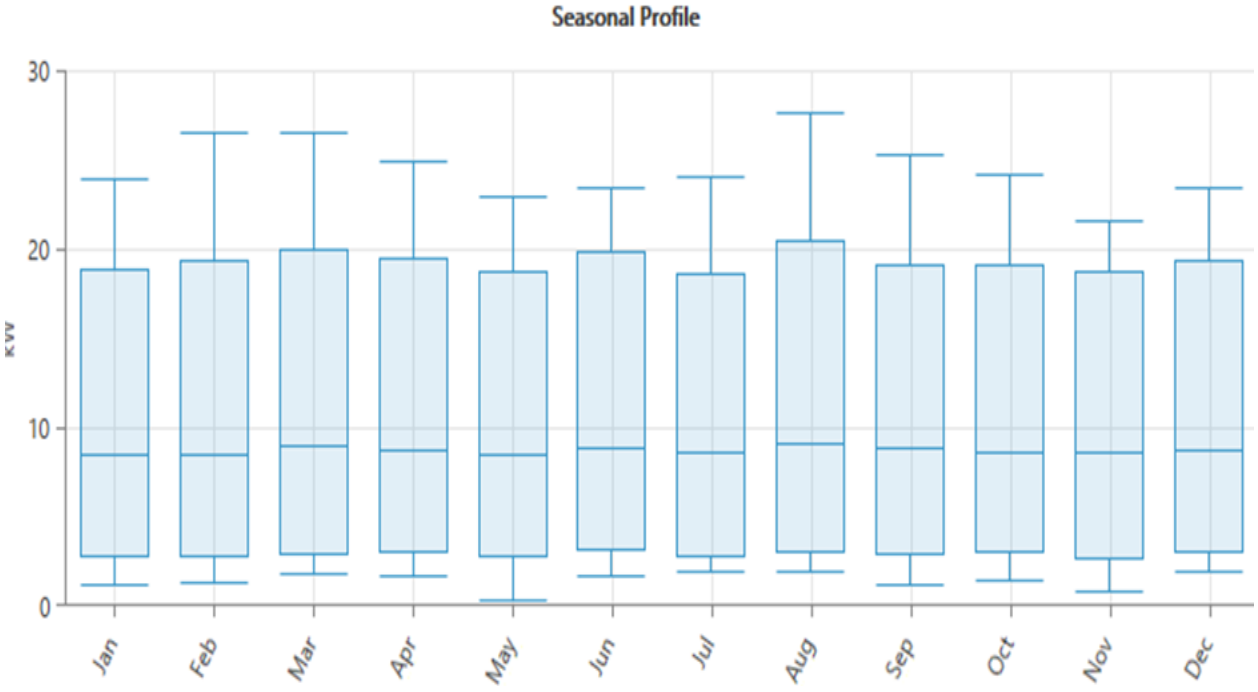

Fig.3 seasonal profile over the year for considered test system

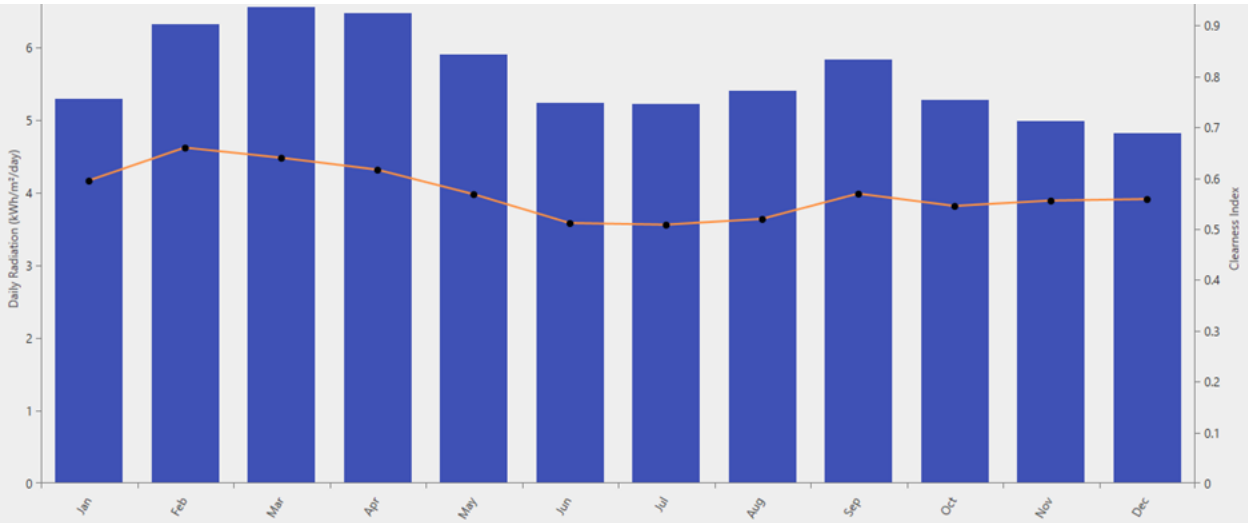

Fig.4 Solar GHI of the considered test system

This figure 4 depicts the monthly variation of solar radiation in kWh/day. Which is represented in blue bars and the clearness index is represented by the orange line with black dots. Its the overview of solar energy potential and atmospheric condition over the year. Daily solar radiation in February, March and September. In contrast the months of June, July and august it receives lowest solar radiation due to cloudy weather. The clearness index remains same between 0.5 and 0.7throughout the year. Both solar radiation and atmospheric condition are their peak during February, March and September. These insights are important for effective solar design and performance optimization.

2.4 Considered test system resources

2.4.1 Photovoltaic system

By providing the DC-BUS via green power, the solar power source integrates green power into the electrical infrastructure. Eq. (1) below can be used to compute the clean power production: The equation 1&2 is referred in [19]

is referred in

$$P_{Pv} = y_{Pv} f_{Pv} \left(\frac{G_T}{G_{T,\mathrm{stc}}}\right)\left[1 + \alpha_{\mathrm{p}}\left(T_{\mathrm{c}} - T_{\mathrm{c,stc}}\right)\right] \quad (1)$$

$$T_{\mathrm{c}} = \left(\frac{T_{\alpha} + (T_{\mathrm{c},noct} - T_{\alpha,noct})\left(\frac{G_T}{G_{T,noct}}\right)}{1 + (T_{\mathrm{c},noct} - T_{\alpha,noct})\left(\frac{G_T}{G_{T,noct}}\right)}\right) * \left(\frac{1 - (\alpha_{mp,stc})\left(\frac{1 - \alpha_p T_{\mathrm{c},stc}}{\tau_{\alpha}}\right)}{\frac{\alpha_{p\eta_{\mathrm{mp}},stc}}{\tau_{\alpha}}}\right) \quad (2)$$

2.4.2 Battery

An individual battery is defined by HOMER's computational framework as an appliance that has a constant energy efficacy and the ability to maintain a specific quantity of electricity, which is called DC power.The eqn 3 is referred in [20]

$$N_{battery} = \frac{\varepsilon_d * n_d}{V_{battery} * Ah * DOD} \quad (3)$$

2.4.3 Diesel Generator

The generic DG unit with a standard capacity of 12kVA is connected. Fuel prices are a major factor in the expenses associated with running and sustaining diesel generators. Consequently, the price of the sensitivity analysis takes fuel into account.

3 Mathematical Expressions

3.1 Evaluation Metrics:

3.1.1 MSE

An additional statistic, known as the mean square error (MSE), is utilized to evaluate the difference between anticipated and actual values.

$$MSE=\frac{1}{n}\sum_{i=1}^{n}(g_{i-}\ \hat{g}_i)\text{^}2 \quad (4)$$

Where, n=sample size , g_i=actual value and $\hat{g}_i$=Predicted value

3.1.2 RMSE

$$RMSE=\sqrt{(\frac{1}{n}\sum_{i=1}^{n}(g_{i-}\ \hat{g}_i)\text{^}2} \quad (5)$$

3.1.3 R^2

An R2 = 1 indicates the regression method with the highest degree of excellence.

$$R^2=1-\frac{\sum_{i=1}^{n}(g_{i-}\ \hat{g}_i)\text{^}2}{\sum_{i=1}^{n}(g_{i-}\ \hat{\hat{g}}_i)\text{^}2} \quad (6)$$

4 Evaluation factors

4.1 Renewable fraction

The fraction of power derived from clean sources that is delivered to the demand is known as the renewable fraction.

$$f_r = 1 - \frac{E_{nonren}+h_{nonren}}{E_{served}+h_{served}} \quad (7)$$

4.2 LCOE

Using Equation (8), the LCOE determines the average price for the framework per kWh of electricity.

$$LCOE=\frac{c_{ann,tot}}{E_{primary,\mathcal{A}c}+E_{Primary,\mathcal{D}c}+E_{gridsales}} \quad (8)$$

5 Homer-Pro outcomes

Table 1 displays edge matrix multi-national company techno-enviro-economic results using the HOMER-PRO applications. To determine the array's power ratio and cost, the technological and financial parts of the forecast method employ the RF and LCOE, accordingly. The results of Homer Pro are used as input data for the several machine-learning methods.

Table1 Best Possible outcome of HES from Homer tool

ON GRID SYSTEM	
Technical	**Best Possible outcome**
Dispatch Strategy	CC
Photovoltaic Array (kW)	16

DieselGenerator (kWh)	16
Number of batteries	17
Converter	7
Capital Cost of PV (₹)	500000
Photovoltaic Production (kWh/y)	29494
RF (%)	26.1
Fuel Consumption (L/yr.)	25599
ExcessElectricity (kWh/y)	879
Unmet Load (kWh/y)	0
CS (kWh/y)	0
Environmental	**Best Possible outcome**
Carbon di oxide (kg/yr.)	55542
Carbonmonoxide (kg/yr.)	583
Unburned HC (kg/yr.)	19.6
ParticulateMatter (kg/yr.)	31.3
SulphurO_2 (kg/yr.)	189
Nitragenoxide (kg/yr.)	524
Economic	**Best Possible outcome**
Initial cost (₹)	1.3M
Operating Cost (₹/yr.)	206424
NPC (₹)	3.54M
LCOE (₹)	2.51

6 Estimating data with machine learning techniques

The on-grid considered test system homer results are contradictory to identify the optimal configuration of the system. so that this issue can be avoided using machine learning algorithm is to predict the optimal configuration of the system .In the MATLAB environment, more than 2000 data mixes were carefully assessed using machine learning techniques.

6.1 Methods of Machine Learning in RF Anticipating

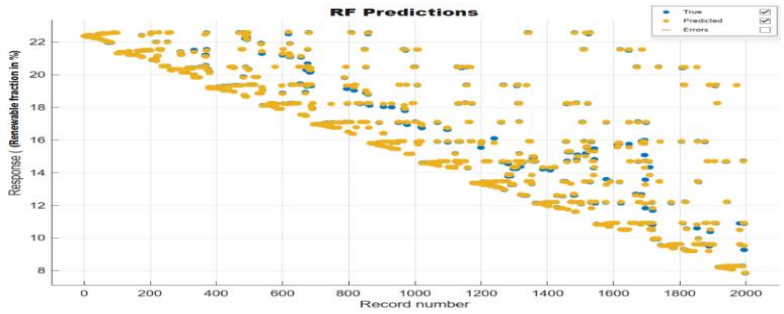

Fig.5 Response plot using optimizable GPR algorithm for RF

Comparing the true and predicted values of the renewable percent (RF) for a set of records, this plot looks to be a scatter plot in Fig.5. The record number, which ranges from 0 to 2000, is represented by the x-axis, while the response (RF in%) is represented by the y-axis. The actual values of RF are indicated by a blue dot, while the predicted values are indicated by orange dots. The predicted values of RF are indicated by orange dots, whereas the actual values of RF are indicated by blue dots. Plotting the record number against the renewable fraction reveals a negative association, with the true and forecasted values having a similar decreasing trend. Although the broad trend is represented, there is a spread around the genuine values by the anticipated values, showing some prediction mistakes. The blue and orange dots aligning suggest that the prediction model estimates the renewable fraction with a reasonable degree of accuracy.

Fig.6 illustrates the comparison between the real and forecasted values of renewable fractions of the system. The X-axis indicates the real values of the RF in percentage and y-axis indicates the forecasted values of RF in percentage. The data points are mentioned by the blue dot. The black dashed line depicts the ideal scenario, where both the expected and actual outcomes are equal. The algorithm would have made perfect forecasting if every point fell on this line. The great degree of accuracy of the model employed to forecast the renewable fraction is indicated by the closed match between the anticipated and actual values along the ideal dashed line in this plot. The model demonstrates reliability and effectiveness for this task, as evidenced by the minimal dispersion of data points around the line, indicating low prediction errors.

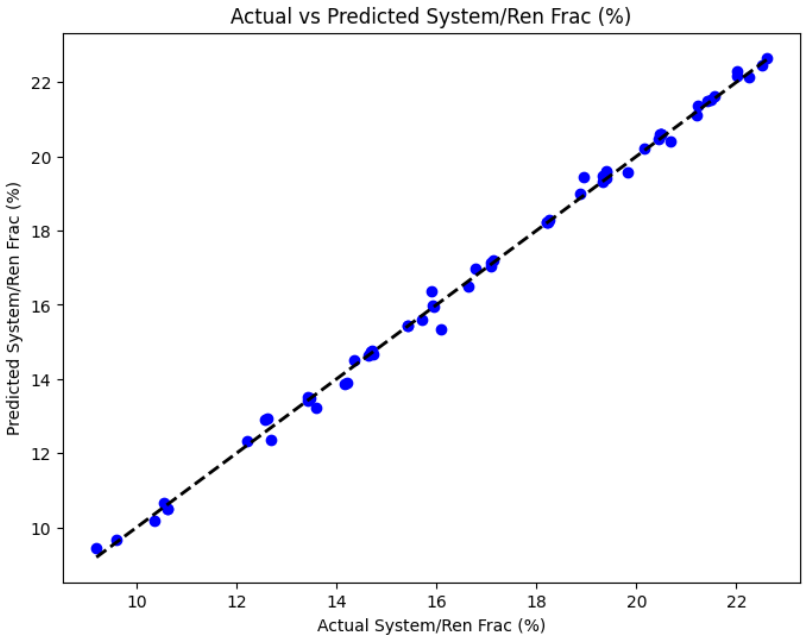

Fig.6Scatter plots of Predicted RF versus actual RF

Table.2 Evaluation of the COE prediction framework using various machine learning techniques

Types of regression training Approaches	Root Mean Square Error	R^2	Mean Square Error	Mean Average Error	Training Time in sec
Linear Regression(LR)	0.076207	0.87	0.005807	0.0489	2.9103
Integer LR	0.075709	0.87	0.005732	0.04755	2.309
Robust LR	0.087889	0.83	0.007722	0.039904	3.2752
Stepwise LR	0.075754	0.87	0.005739	0.047829	3.719
Tree (Fine)	0.019754	0.99	0.00039	0.01119	2.5422
Tree (Medium)	0.026382	0.96	0.000696	0.015592	1.0371
Tree(Coarse)	0.040893	0.96	0.001679	0.026019	0.63562
Optimizable Tree	0.018842	0.99	0.000355	0.010124	18.064
Linear SVM	0.083481	0.85	0.006969	0.040579	15.213
Quadratic SVM	0.057126	0.93	0.003263	0.032207	183.22
Cubic SVM	0.095256	0.8	0.009074	0.055272	370.42
SVM (Fine Gaussian)	0.024861	0.99	0.000618	0.022401	1.7061
SVM (Medium Gaussian)	0.025287	0.99	0.000639	0.020075	2.7284
SVM (Coarse Gaussian)	0.068149	0.9	0.004376	0.034269	1.4293
Optimizable SVM	0.21228	0	0.045065	0.18347	361.01
SVM kernel	0.024091	0.99	0.00058	0.02081	364.64
Least Square Kernel	0.021982	0.99	0.000483	0.014232	361.86
Boosted Tree Ensemble	0.10856	0.74	0.011785	0.10543	162.18
Bagged Tree Ensemble	0.020861	0.99	0.000435	0.011917	353.76
optimizable Ensemble	0.021795	0.99	0.000475	0.013585	358.5
Narrow Neural Network	0.022953	0.99	0.000527	0.015259	359.23
Medium NN	0.018638	0.99	0.000347	0.011192	357.99
Wide NN	0.018434	0.99	0.00034	0.010495	356.92
Bilayered NN	0.020668	0.99	0.000427	0.013179	356.08
Trilayered NN	0.01884	0.99	0.000355	0.011207	355.29
Optimizable NN	2.0748	-94.52	4.3046	2.0639	492.54
Optimizable GPR	0.01827	0.99	0.000334	0.10378	9600.1

The RF (Renewable fraction) of an HRES can be estimated using a predictive model built using a variety of machine learning techniques, including ensemble methods, Gaussian Process Regression, Decision Trees, Support Vector Machines, Neural Networks, and Kernel methods.

Table 3 contains specifics on these techniques. Considerable acceptance with simulation data is shown by most machine learning techniques used for RF prediction. Relatively short training periods are observed for the linear SVM, coarse Gaussian SVM, kernel SVM, thin neural network (NN), Tri layered NN, fine tree, and medium coarse tree regression models; the maximum training period is 29.46 seconds. On the other hand, 11338 seconds is the maximum amount of training time required by the optimizable Gaussian process regression technique. The training times for ensemble approaches, NN regression models, cubic SVM, quadratic SVM, and optimizable SVM range from 33 to 45 seconds. Out of all the models, the integer linear regression model has the quickest training time, taking only 0.3512 seconds to complete. Among the assessed models, the optimizable Gaussian Process Regression (GPR) model shows improved accuracy in predicting RF with R^2 value of 1.With the lowest RMSE (Root Mean Square Error), MSE (Mean Square Error), and MAE (Mean Absolute Error) values ever tested at 0.01827, 0.001993 and 0.018556in that order, this optimizable GPR model impressively achieves the greatest accuracy of all training procedures. Thus, the optimal GPR model is the optimum choice for RF prediction in the HRES based on the response plot and the comparison of predicted and real RFs (Fig. 7 and 8, respectively).

6.1.1 Methods of Machine Learning in COE Anticipating

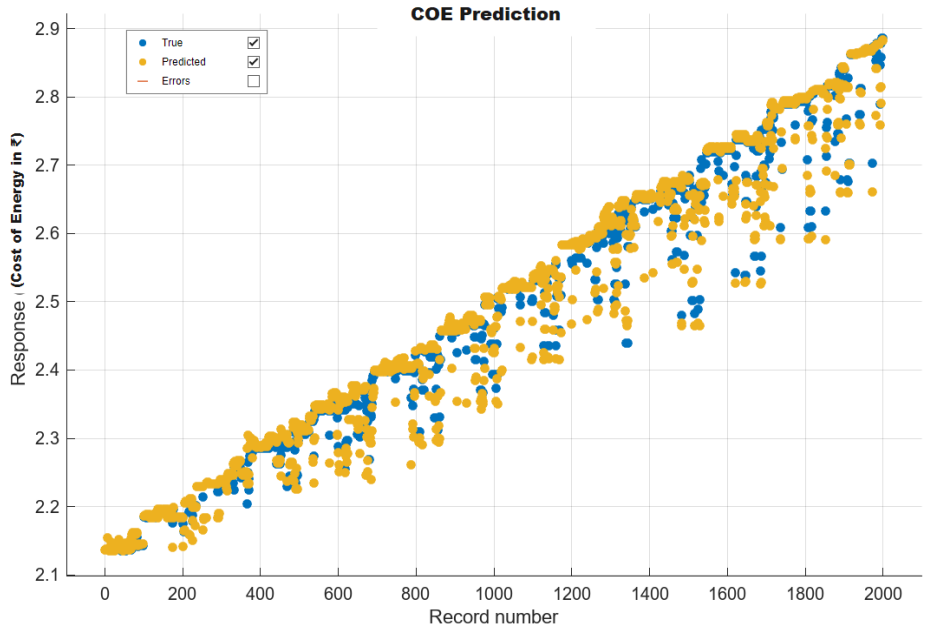

Fig.7 Response plot using optimizable GPR algorithm for COE

The plotin Fig.7compares the actual and estimated values of the Cost of Energy (COE) for a number of records, looks to be a scatter plot. Record numbers, which span from 0 to 2000, are shown by the x-axis, while response values (COE in ₹) are represented by the y-axis. The actual COE values are shown by the blue dot, while the projected COE values are shown by the orange dots.Plotting the record number against the COE reveals a strong positive association, with the true and anticipated values showing a similar increasing trend. The broad trend is well represented, but there is a discernible spread around the genuine values by the predicted values, indicating some degree of prediction error. The blue and orange dots' close alignment indicates that the prediction model is performing reasonably well in estimating the COE.

Fig.8 shows the comparison between the actual and forecasted values of the Cost of Energy (COE) for the system. The X-axis represents the actual COE values in percentage, while the Y-axis represents the forecasted COE values in percentage. The red dots denote the data points, and the ideal scenario, where forecasted and actual values are identical, is illustrated by the black dashed line. The model would have achieved perfect forecasting if all points aligned with this line. The close alignment of the expected and actual

values with the ideal dashed line indicates the high accuracy of the model in forecasting the COE. The model's reliability and effectiveness are demonstrated by the minimal dispersion of data points around the line, reflecting low prediction errors.

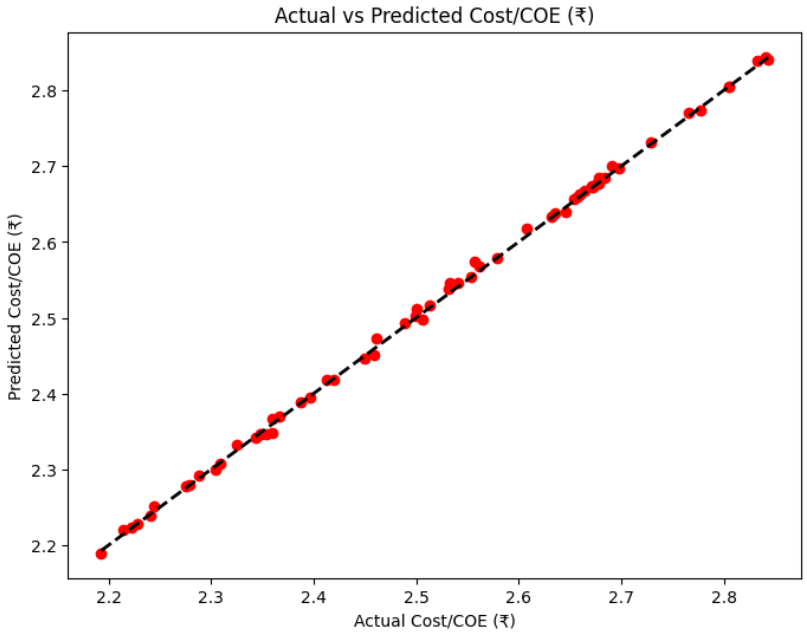

Fig.8 Scatter plots of Predicted COE versus actual COE

Table.3 Evaluation of the RF prediction framework using various machine learning techniques

Types of regression training Approaches	Root Mean Square Error	R2	Mean Square Error	Mean Average Error	Training Time in sec
Linear regression(LR)	0.76746	0.97	0.589	0.47484	9.8162
Integer LR	0.76003	0.97	0.57765	0.45743	0.3512
Robust LR	0.8809	0.96	0.77613	0.3676	8.143
Stepwise LR	0.76075	0.97	0.57874	0.45946	9.8907
Fine Tree	0.086069	1	0.0074	0.033195	10.142
Medium Tree	0.2222	1	0.049372	0.082649	2.6136
Coarse Tree	0.45906	0.99	0.21073	0.19407	1.9005
Optimizable Tree	0.069131	1	0.004779	0.02735	45.769
Linear SVM	0.79397	0.96	0.6304	0.43572	12.296
Quadratic SVM	0.57389	0.96	0.32934	0.40746	136.07
Cubic SVM	0.41497	0.99	0.1722	0.35965	134.86
SVM (Fine Gaussian)	0.33489	0.99	0.11215	0.28767	37.449
SVM (Medium Gaussian)	0.32056	0.99	0.10276	0.27922	36.042

SVM (Coarse Gaussian)	0.60392	0.98	0.36472	0.37361	11.638
Optimizable SVM	0.12938	1	0.016739	0.079844	275.95
SVM kernel	0.41489	0.99	0.17213	0.31929	11.67
Least Square Kernel	0.22493	1	0.050595	0.1265	8.8441
Boosted Tree Ensemble	0.716	0.97	0.51266	0.68387	29.46
Bagged Tree Ensemble	0.10717	1	0.011485	0.042869	33.878
optimizable Ensemble	0.10308	1	0.010626	0.072162	111.71
Narrow Neural Network	0.39266	0.99	0.15387	0.18972	5.0978
Medium NN	0.082462	1	0.0068	0.055366	32.716
Wide NN	0.047263	1	0.002234	0.022357	33.878
Bilayered NN	0.095189	1	0.009061	0.060345	56.116
Trilayered NN	0.18244	1	0.033283	0.073119	24.09
Optimizable NN	0.76746	0.97	0.58899	0.47519	227.89
Optimizable GPR	0.04464	1	0.001993	0.018556	11338

A prediction model was built using twenty-seven different types of machine learning approaches to estimate COE (Cost of Energy). The results, which are presented in Table 2, show that most machine learning methods used to forecast COE are significantly in agreement with simulation outcomes. When compared to other techniques, the training times for the linear regression, Tree(fine , medium) optimizable tree, SVM(linear, fine Gaussian, medium Gaussian, and coarse Gaussian) regression models are comparatively quick, with an utmost amount of training time is 18.064 seconds. In contrast, the optimizable Gaussian Process Regression (GPR) technique, with a training time of 9600 seconds, demands the longest. Neural network (NN) models, optimizable SVM, kernel techniques, and cubic SVM require training times ranging from 150 to 492.54 seconds. The Coarse Tree model that requires the least amount of time to train is 0.63562 seconds. The models that employ optimizable GPR models provide the best predictive power for COE. These models are incredibly precise, as evidenced by their coefficient of determination (R^2) of 1. In terms of RMSE, MSE, and MAE the models that employ optimizable GPR models perform better than the other models; the relevant numbers are 0.01827, 0.000334 and 0.10378. Thus, the optimal GPR model is the optimum choice for COE prediction in the HRES based on the response plot and the comparison of predicted and real COEs (Fig.7and 8, respectively).

Conclusion

This study exhibited the optimal hybrid energy configuration for commercial building located in city centre through homer simulation tool and machine learning techniques. The study findings reveals that the integration of grid, solar battery renders the increasing RF of 26.1% .Although it failed to deliver the best technical outcomes, the research discovered that the combination comprising solar PV, grid, battery and DG delivered an affordable LCOE of ₹2.51 million. The Optimizable GPR model, with an outstanding R^2 value of 0.99, achieves the highest accuracy for Levelized Cost of Energy (LCOE) prediction among all training procedures. It also achieves the lowest Mean Absolute Error (MAE), Mean Squared Error (MSE), and Root Mean Squared Error (RMSE), with values of 0.01827, 0.001993, and 0.018556, respectively. In terms of RF prediction, the Optimizable GPR model performs better than others, with R^2 equal to 1 and RMSE, MSE, and MAE values of 0.01827, 0.001993, and 0.018556, respectively. For RF prediction, the Optimizable GPR model is considered the best option. Thus, the framework aids in promoting overall energy performance through technically stable and economically feasible configuration as a solution.

Acknowledgement

The authors of this article would like to express their sincere gratitude to the Madurai-based organization Edge matrix multi- national company. Their assistance and collaboration have been crucial to the accomplishment of this study endeavor. Furthermore, the authors would like to thank Thiagarajar College of Engineering, Madurai, for funding this research project through the Thiagarajar Research Fellowship (File No. TCE/TRF-Jan2022/07), which has been crucial to its advancement.

Reference

1. International Energy Agency. Energy efficiency: Buildings. The global exchange for energy efficiency policies, data and analysis. (accessed Jun. 01, 2023).
2. Stram BN. Key challenges to expanding renewable energy. Energy Policy. 2016 Sep 1;96:728-34.
3. Adnan M, Tariq M, Zhou Z, Poor HV. Load flow balancing and transient stability analysis in renewable integrated power grids. International Journal of Electrical Power & Energy Systems. 2019 Jan 1;104:744-71.
4. European Comission. Energy communities. https://energy.ec.europa.eu/to pics/markets-and-consumers/energy-communities (accessed Jun. 01, 2023).
5. Jamian JJ, Mustafa MW, Mokhlis H, Baharudin MA. Simulation study on optimal placement and sizing of battery switching station units using artificial bee colony algorithm. International Journal of Electrical Power & Energy Systems. 2014 Feb 1;55:592-601.
6. Baruah A, Basu M, Amuley D. Modeling of an autonomous hybrid renewable energy system for electrification of a township: A case study for Sikkim, India. Renewable and Sustainable Energy Reviews. 2021 Jan 1;135:110158.
7. Houben N, Cosic A, Stadler M, Mansoor M, Zellinger M, Auer H, Ajanovic A, Haas R. Optimal dispatch of a multi-energy system microgrid under uncertainty: A renewable energy community in Austria. Applied Energy. 2023 May 1;337:120913.
8. Orehounig K, Evins R, Dorer V. Integration of decentralized energy systems in neighbourhoods using the energy hub approach. Applied Energy. 2015 Sep 15;154:277-89.
9. Vohra K, Vodonos A, Schwartz J, Marais EA, Sulprizio MP, Mickley LJ. Global mortality from outdoor fine particle pollution generated by fossil fuel combustion: Results from GEOS-Chem. Environmental research. 2021 Apr 1;195:110754.
10. Shakeel MR, Mokheimer EM. A techno-economic evaluation of utility scale solar power generation. Energy. 2022 Dec 15;261:125170.
11. Kusakana K, Munda JL, Jimoh AA. Feasibility study of a hybrid PV-micro hydro system for rural electrification. InAFRICON 2009 2009 Sep 23 (pp. 1-5). IEEE.
12. Murugaperumal K, Srinivasn S, Prasad GS. Optimum design of hybrid renewable energy system through load forecasting and different operating strategies for rural electrification. Sustainable Energy Technologies and Assessments. 2020 Feb 1;37:100613.
13. Ahmed W, Ansari H, Khan B, Ullah Z, Ali SM, Mehmood CA, Qureshi MB, Hussain I, Jawad M, Khan MU, Ullah A. Machine learning based energy management model for smart grid and renewable energy districts. IEEE Access. 2020 Oct 9;8:185059-78.
14. Zohuri B. Hybrid energy systems: Driving reliable renewable sources of energy storage. Springer; 2017 Nov 25.
15. Houssein EH, Ibrahim IE, Kharrich M, Kamel S. An improved marine predators algorithm for the optimal design of hybrid renewable energy systems. Engineering Applications of Artificial Intelligence. 2022 Apr 1;110:104722.
16. Tezer T, Yaman R, Yaman G. Evaluation of approaches used for optimization of stand-alone hybrid renewable energy systems. Renewable and Sustainable Energy Reviews. 2017 Jun 1;73:840-53
17. Qiao Z, Li L, Zhao X, Liu L, Zhang Q, Shili H, Atri M, Li X. An enhanced Runge Kutta boosted machine learning framework for medical diagnosis. Computers in Biology and Medicine. 2023 Jun 1;160:106949.

18. Giglio E, Luzzani G, Terranova V, Trivigno G, Niccolai A, Grimaccia F. An efficient artificial intelligence energy management system for urban building integrating photovoltaic and storage. IEEE Access. 2023 Feb 22; 11:18673-88.
19. Ali F, Ahmar M, Jiang Y, AlAhmad M. A techno-economic assessment of hybrid energy systems in rural Pakistan. Energy. 2021 Jan 15;215:119103.
20. Elomari Y, Mateu C, Marín-Genescà M, Boer D. A data-driven framework for designing a renewable energy community based on the integration of machine learning model with life cycle assessment and life cycle cost parameters. Applied Energy. 2024 Mar 15;358:122619.